SAND2018-5578C

PV Inverter Fault Response Including Momentary Cessation, Frequency-Watt, and Virtual Inertia

Brian J. Pierre[1], Mohamed E. Elkhatib[2], and Andy Hoke[3]

[1]Sandia National Laboratories, Albuquerque, NM, USA, [2]S&C Electric Company, Chicago, IL, USA, [3]National Renewable Energy Laboratory, Golden, CO, USA

***Abstract* — This paper presents two photovoltaic (PV) inverter control methods and an analysis of the two under a significant three-phase transmission line fault contingencies in the Hawaiian island of Oahu power system. Simulations are presented for the two control methods on the island power system with a high penetration of PV generation, approximately 40% of the total. The two control methods discussed are similar: one is a proportional frequency-watt controller, and the second is a proportional-derivative controller, a frequency-watt controller with virtual inertia. Both methods can be beneficial for fast frequency support. The inverter model also emulates inverter fault response including "momentary cessation" and recovery during low voltage events. The study presented in this paper utilizes a validated power system model of the Hawaiian island of Oahu, modified to include PV resources with the two custom developed control models. Dynamic simulations with PSS/E are presented during a significant transmission line three-phase fault contingency. Simulations are presented with and without PV reserve margin. In addition, a parameter sensitivity analysis is presented for the control methods. Results indicate both methods can significantly improve system response during fault events. Findings indicate that transmission faults can produce severe frequency events, and that fast recovery from momentary cessation is crucial to mitigate severity.**

***Index Terms* — Smart inverter, frequency-watt function, photovoltaic, PV, frequency control, virtual inertia, momentary cessation, inverter control**

I. Introduction

With renewable energy portfolio standards for many states and countries around the world, and decreasing prices for solar energy technologies, photovoltaic (PV) penetration levels continue to rise. As PV starts to displace traditional generation, it is important for PV to help support grid functions traditionally performed by conventional synchronous machines. Such support functions include frequency support, reactive power support, and transient voltage ride through. Recent research and system tests have shown that PV inverters, if controlled correctly, can provide some of these services. For example, [1-4] discuss the use of frequency–watt functionality under generation and load trips for fast frequency support. [5] looks at the optimal frequency-watt curve given certain penetration levels. [6-7] discuss grid forming inverters. [8-10] analyze inverter control methods for voltage support with Volt/Var, Volt/Watt, and fixed power factor controls. [11] analyzes virtual inertia, and [12] discusses communication latency on virtual inertia controls. In all of these cases, for PV to provide these services, the smart inverter must be able to control the active and/or reactive power output of the PV system quickly.

More recently, inverter vendors have started to include grid support functions in response to new standards and requirements from some utilities. In fact, some frequency-watt capabilities have started to become implemented in the U.S.; Hawaiian Electric recently became the first U.S. utility to require system-wide activation of frequency-watt control [13] based on recommendations from a Department of Energy Grid Modernization Lab Consortium study [14]. The new revision of IEEE Standard 1547 requires that all distributed energy resources (including PV) be capable of several grid support functions including frequency-watt control [15].

The goal of this paper is to analyze two promising PV inverter control methods to improve fast frequency support during transient events. The two control methods are: frequency-watt control (FWC), and hybrid frequency-watt virtual inertia control (FWVIC). Virtual inertia refers to the use of power electronics to emulate physical inertia, and includes inherent measurement and control delays not present in true inertia. Virtual inertia is based on the derivative of the frequency. FWC is available in some inverters today, whereas FWVIC is typically not. As implemented here, both controllers are current-controlled inverter models and include realistic low-voltage response dynamics including momentary cessation of inverter output during very low voltage events, and subsequent recovery dynamics. The two methods are analyzed on a validated power system model of the Hawaiian island of Oahu with approximately 40% PV penetration, and the island can incur instantaneous PV penetration up to 56%. The inverter controllers for the PV resources in the system are implemented using custom user defined models. Dynamic PSS/E simulations are presented during two significant three-phase fault events. Results are shown with different reserve margins and a parameter sensitivity is analyzed. Results from this project helped the Hawaiian Electric Companies implement frequency-watt functionality on the inverters that had this functionality.

The rest of this paper is organized as follows: Section II explains the two control models in detail, Section III explains the momentary cessation control. Section IV shows results analyzing the two control models during the fault contingencies. Section V presents a parameter sensitivity analysis and Section VI describes the conclusions and future work.

Brian J. Pierre is a senior member of technical staff in the power systems research group at Sandia National Laboratories, bjpierr@sandia.gov.

Sandia National Laboratories is a multimission laboratory managed and operated by National Technology and Engineering Solutions of Sandia, LLC, a wholly owned subsidiary of Honeywell International, Inc., for the U.S. Department of Energy's National Nuclear Security Administration under contract DE-NA0003525. The views expressed in the article do not necessarily represent the views of the U.S. Department of Energy or the United States Government.

II. Frequency-Watt and Frequency-Watt Virtual Inertia Controllers

Grid following inverters (i.e. nearly all grid-connected inverters today) are current controlled inverters and in a transient stability analysis program can be modelled as a controlled power source. Typically, grid following inverters are controlled in the *dq*-frame (if three-phase) and synchronized with the grid voltage using a phase locked loop (PLL), and contain an inner current control loop and an outer power control loop. The output power is controlled to its maximum level in most circumstances to get the most energy possible out of the PV panel. However, as PV penetration increases, the output power may be controlled to include a reserve margin to allow head room for other grid services, such as fast frequency support during a generation trip.

A. Frequency – Watt Controller

Frequency-watt control (FWC) has been studied in [1-6, 14], but not during faults. The frequency-watt curve in Fig. 1 should be steep enough to allow the inverter to quickly react to the frequency event. However, as shown in [1, 4, 14], increasing the steepness of the FW function could result in frequency oscillations. Therefore, there is a trade-off between response magnitude and unwanted oscillations. In Fig. 1 f_o is the nominal system frequency, P_{set} is the normal power output of the inverter without frequency-watt enabled. K_{uf} and K_{of} are the slopes of the upward and downward power response. P_{min} is the minimum allowed power output of the inverter, P_{avai} is the maximum power available, and db_{of} and db_{uf} are the deadband limits for the frequency-watt function.

The frequency-watt controller (Fig. 2) modulates power in proportion to frequency deviation. In Fig. 2, f is the system frequency, and f_{meas} is the same as f, but with a time constant T_1 approximating the PLL response time. ΔP_{FW} is the change in the power output from the proportional (FW) part of the controller. P_{ref} is the output power command to the power controller.

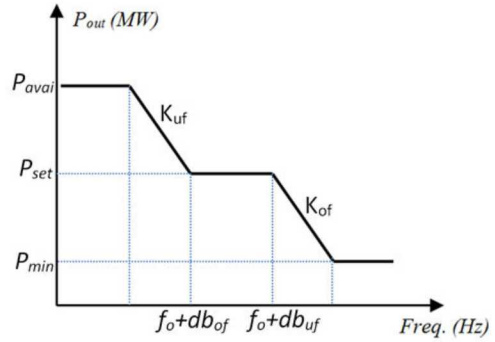

Fig. 1. The frequency-watt function

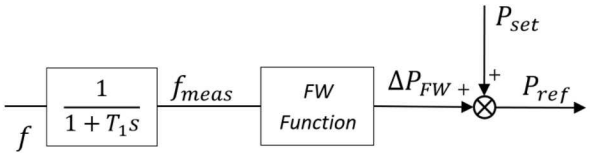

Fig. 2. The frequency-watt distributed PV model

B. Frequency – Watt Virtual Inertia Controller

The FWVIC model includes the frequency-watt controller presented in Section II.A with an additional component based on the derivative of the frequency, i.e. virtual inertia. The virtual inertia portion of the control allows for quicker response to events and therefore better fast frequency support, while minimizing frequency oscillations. Interconnection standards and inverters available today do not typically include FWVIC.

The FWVIC model is in Fig. 3, and rather than a proportional FW controller, the FWVIC is a proportional-derivative (PD) controller. Fig. 3 includes many elements which were explained in Fig. 2 with the addition of: T_2, the virtual inertia filter time constant; K_2, is the virtual inertia gain; and ΔP_{SI}, the change in the power output from the derivative part of the controller, i.e. the virtual inertia part of the controller. Note there can also be deadband limits for the FWVIC. The values used for simulations for both the FWC and the FWVIC are in Table I.

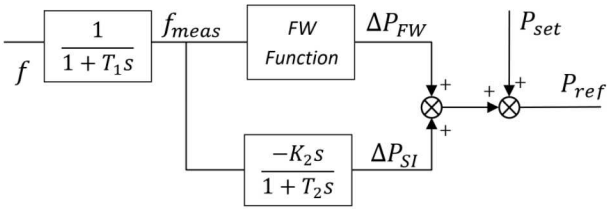

Fig. 3. The frequency-watt with virtual inertia distributed PV controller

III. Current Limiter Logic

To be more realistic, the FWC and FWVIC models include a current limiter for when the terminal voltage drops below a certain threshold; also representing the inverter behavior known as *momentary cessation*, as specified in IEEE 1547-2018 [15]. If the terminal voltage drops too low, the inverter model would request a significant amount of current which may be beyond the transistors' current limits. Fig. 4 shows the block diagram of the current limiter. P_{ref} is the output from Fig. 2 or Fig. 3, V_t is the measured AC voltage, I_{ref} is the current requested that may need to be limited, T_3 is the inverter response time, and P_{out} is the final output power of the smart inverter.

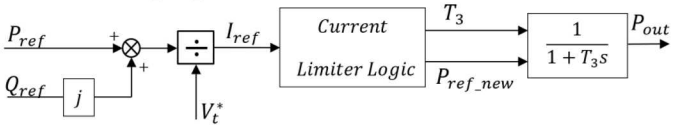

Fig. 4. The current limiter block diagram

The current limiter logic in Fig. 4 is broken into five cases:

1. If $I_{ref} > I_{max}$:
   $T_3 = T_{limiter}$, $P_{out} = \sqrt{(I_{max} * |V_t|)^2 - Q_{ref}{}^2}$, $I_{limit} = 1$
2. If $I_{ref} < I_{max}$ & $I_{limit} = 1$:
   $T_3 = T_{recovery}$, $P_{out} = P_{ref\_new}$, *if* $P_{out} > P_{recovery}$: $I_{limit} = 0$
3. If $V_t < V_{lv}$:
   $T_3 = T_{limiter}$, $P_{out} = 0$, $V_{dip} = 1$
4. If $V_t > V_{lv}$ & $V_{dip} = 1$:
   Wait for $T_{delayRecovery}$, then let: $T_3 = T_{recovery}$,
   $P_{out} = P_{ref\_new}$, *if* $P_{out} > P_{recovery}$: $V_{dip} = 0$
5. $T_3 = T_3$, $P_{out} = P_{ref\_new}$ (normal operation case)

TABLE I
The Parameters in the FWVIC Model

Default value	Name	Comments
0.05	T_1	Frequency measurement time constant (PLL response time)
1	K_1	Flag to enable/disable FW function (1 to enable)
0.01	T_2	Virtual inertia differentiation time constant
1	K_2	Virtual inertia gain
0.5	T_3	Inverter power time constant (normal operation)
0.05	K_{of}	Over-frequency droop (pu Hz / pu power)
0.05	K_{uf}	Under-frequency droop (pu Hz / pu power)
0.1	db_{of}	Over-frequency deadband (Hz)
0.1	db_{uf}	Under-frequency deadband (Hz)
0	P_{max} % available headroom	For example: P_{max} = 10% means that the PV is operating 10% below its available power.
0	P_{min} (p.u. of rated power)	For example: P_{min} = 10% means that the PV has to maintain output of 10% of the rated power or be shutdown.
1.1	I_{max}	Maximum inverter current (pu)
0.5	V_{lv}	Low voltage limit (if $V < V_{lv}$: inverter will cease to inject power but stay connected)
0	$T_{limiter}$	Current limiter time constant (If $I>I_{max}$, the inverter will be modelled using this time constant) typically much faster than T_3.
0.03	$T_{recovery}$	Inverter recovery time constant (when I becomes less than I_{max} after voltage recovery, inverter output is controlled using this time constant until the power reaches $P_{recoveryLimit}$
0.9	$P_{recovery}$	Inverter recovery power limit (once the inverter output recovers above this value, the inverter is controlled by the time T_3 time constant)
0	$T_{delayRecovery}$	Time delay before inverter starts recovering from voltage dip after the voltage has recovered

Case 1 is where the controller is requesting more current than allowed, where I_{max} is the maximum current the inverter can supply, $T_{limiter}$ is the inverter response time and the time it takes to limit the current, and I_{limit} is a Boolean to determine if the limit has been reached. Case 2 is where the controller *was* requesting more current than allowed, but has recovered, and can resume normal operation if P_{out} is greater than the $P_{recovery}$ limit. $T_{recovery}$ is the inverter response time during the recovery stage. Case 3 is where the voltage at the AC terminal is less than the momentary cessation limit, V_{lv}, and V_{dip} is a Boolean to determine if the limit has been reached. Case 4 is where the voltage dropped below V_{lv}, but has recovered; the inverter power recovery starts after $T_{delayRecovery}$, and normal operation resumes once P_{out} surpasses the $P_{recovery}$ level. Lastly, Case 5 is normal operation.

The parameters studied in this abstract are in Table I. The only change between the FWC and the FWVIC in Table I is that during FWC functionality, the virtual-inertia part is turned off by changing the constant gain K_2 to zero.

IV. Inverter Analysis Simulation Studies

The system studied in this paper is the dynamic model of the Hawaiian island of Oahu. The system has 460 MW of PV generation which supplies 40% of the peak load. The simulation utilizes PSS/E for the dynamic studies. A custom user defined model (UDM) was developed in PSS/E for the FWC and FWVIC. The original system was modified to include the UDM for 410 MW of the PV; the rest is considered legacy PV without the ability to incorporate the smart inverter controls or momentary cessation. The proportion of frequency-responsive PV to legacy PV has been increased for study purposes; this is likely an over-estimate of the amount of smart PV on Oahu in any near-term scenario. Under the base case with no smart inverter control method applied (legacy PV), it is assumed the inverters do not have low voltage ride-through, and once the voltage drops below 50% the inverter will trip within 0.16 sec. as required by IEEE Standard 1547-2003 [16]. Additional information on the PSSE model can be found in [14].

A. *Generation or Load Trip*

Although this paper focuses on frequency-watt and virtual inertia response to transmission system faults, two contingencies are shown for a generation trip with 20% PV reserve and a load trip with no reserve. Further load trip analysis for FWC and FWVIC is shown in [1, 2, 4], and generation trip analysis for the FWC is in [2, 4, 13]. These results are to show the inverters behave as expected and benefit the system during load or generation loss. Fig. 5 shows the system frequency during a 200 MW conventional generation trip, 17.2% of the system generation. Fig. 6 shows the system frequency during a 62 MW load trip, 5.3% of the island system load.

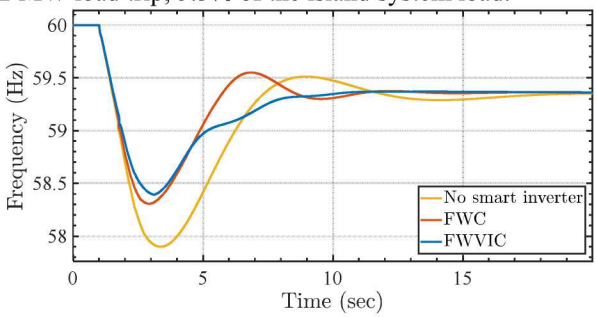

Fig. 5. System frequency during a 200 MW generation trip with and without inverter control.

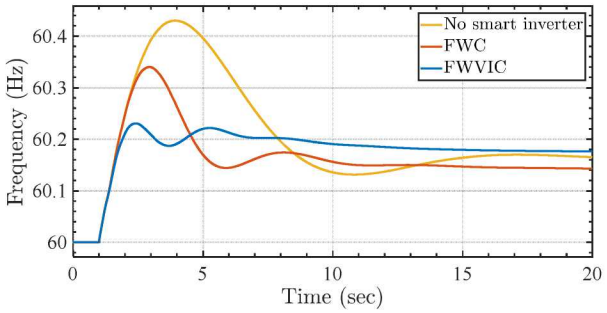

Fig. 6. System frequency during a 62 MW load trip with and without inverter control.

B. *Three Phase Fault*

This contingency compares the control methods during a three-phase fault on a high voltage transmission line. The fault causes a low voltage case where the legacy PV in the system trips offline. This is approximately 50 MW of PV. The fault occurs at time t=1 sec. The ~50 MW of legacy PV trip offline. The circuit trips at t=1.083 seconds (five cycles), recloses again at t=1.5 seconds, and trips again after five cycles and remains open. Fig. 7 shows the frequency with no reserve, and Fig. 8 shows the PV output power. Notice that the FWC and momentary cessation in Figures 7 and 8 are identical; this is because there are no reserves and the frequency is almost entirely below 60 Hz, therefore the FWC is controlling the PV to output its maximum power which is the same as with just momentary cessation. Fig 9 and 10 show the frequency and PV output power with 20% reserve, and there is a noticeable improvement with the control methods enabled.

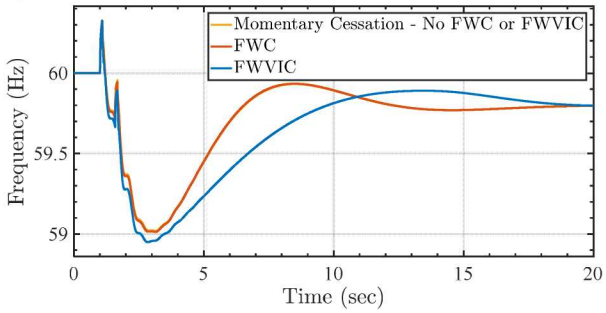

Fig. 7. The system frequency response during a transmission line three-phase fault with different inverter control methods applied, with no PV reserves.

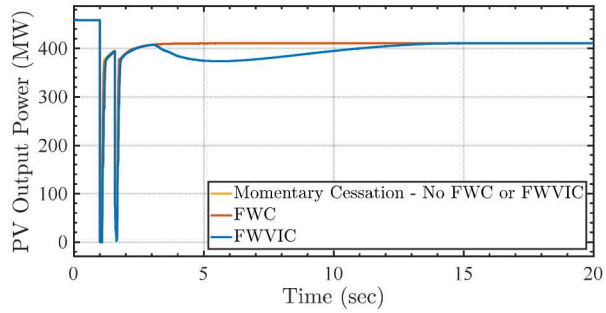

Fig. 8. The power output of the aggregate PV during a transmission line three phase fault with different inverter control methods, with no PV reserves

If none of the PV had ride-through enabled, all 460 MW of PV would trip offline, and there would be a drastic frequency dip causing tripping of conventional generators and an island-wide blackout. This points toward a key take-away, which is that during faults, the most important aspect for smart inverter control methods is that they have voltage/frequency ride-through capabilities that are based off system studies. It would actually be preferable from a bulk system perspective for the PV to ride-through without momentary cessation. Momentary cessation is the result of a compromise between distribution needs and transmission needs. The distribution operators would prefer the PV trip due to islanding and protection concerns, and the transmission operators would prefer it operate continuously.

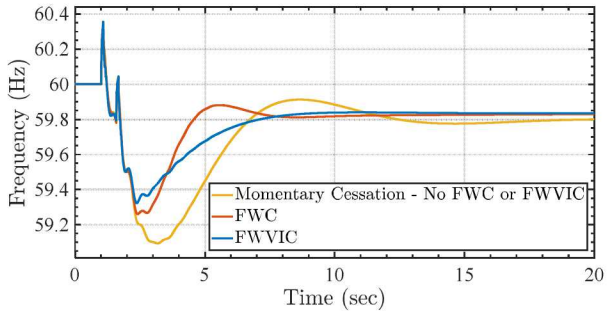

Fig. 9. The system frequency response during a transmission line three phase fault with different inverter control methods applied, with 20% reserves.

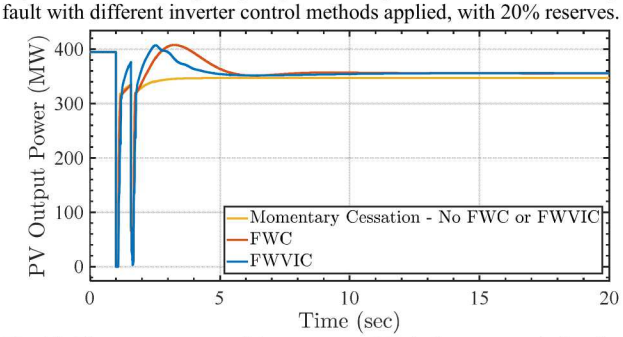

Fig. 10. The power output of the aggregate PV during a transmission line three phase fault with different inverter control methods applied, with 20% reserves.

V. Parameter Sensitivity Analysis

This section shows the frequency of the system during the three-phase fault presented in Section IV.B., with modified parameters from Table I. This also shows the sensitivity analysis for FWVIC for the trip of legacy PV generation due to the fault. For actual implementation of either the FWC or FWVIC models, it is likely the parameters will be tuned and may significantly differ from those in Table I. This section should help determine how changes to each parameter would affect the system response.

A. *Amount of Reserves*

Reserves are added for each case for the controllable PV from 0% to 30%. The greater the reserves, the quicker the system is to recover from the under-frequency event.

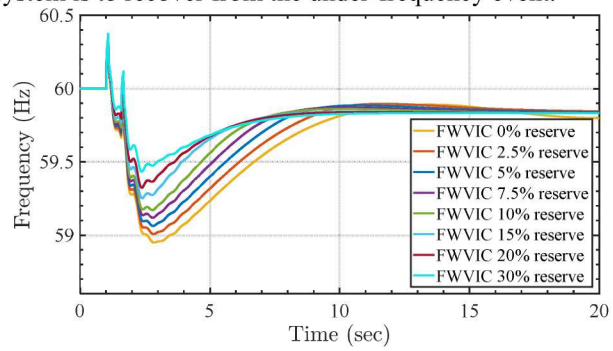

Fig. 11. The system frequency response during a transmission line three-phase fault when PV includes FWVIC and momentary cessation, with different PV reserve margins.

B. *Frequency-Watt Droop* (K_{uf}, K_{of})

For a generation trip and the fault studied in this paper, the droop only very minorly affects the response unless there is reserve because PV without reserve provides no primary response for frequencies below 60 Hz. So, a parameter sensitivity analysis for this section is shown for the 20% reserve margin case. The lower (steeper) the droop, the quicker the response, however, per [1, 4, 14], too steep a droop could result in frequency oscillations. Therefore, there is a trade-off between response magnitude and unwanted oscillations.

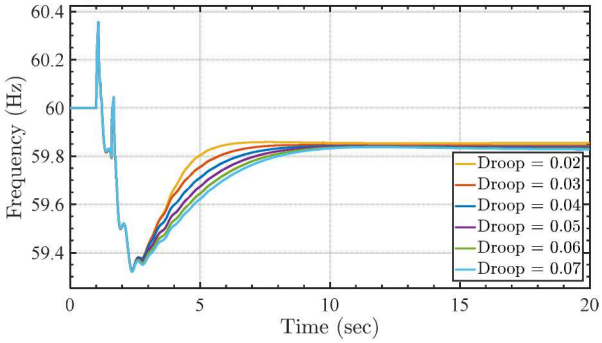

Fig. 12. The system frequency response during a transmission line three-phase fault when PV includes FWVIC and momentary cessation, with different FWC droop.

C. *Virtual-Inertia Gain* (K_2)

In this contingency, the FWVIC has a slower recovery than the FWC from the under-frequency event; this is due to the positive slope in the recovery (starting around t=3 sec. in Fig. 13). The positive slope causes the virtual inertia control to curtail some of the PV output, hence the slower but better-damped recovery with higher K_2 gain.

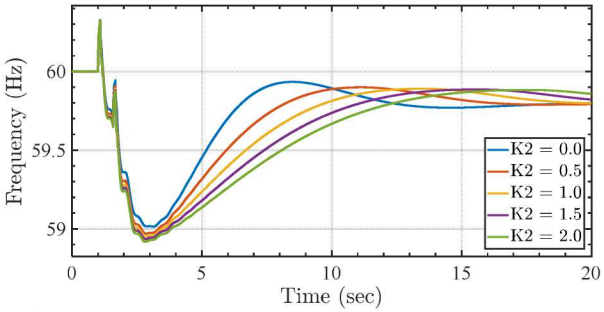

Fig. 13. The system frequency response during a transmission line three-phase fault when PV includes FWVIC and momentary cessation, with different virtual inertia gain. Note K_2 = 0.0 is just FWC.

D. *Recovery Time Constant* ($T_{recovery}$)

The recovery of the PV output power after momentary cessation is extremely important and should be very fast to minimize impacts on system stability. The default time constant is 0.03 seconds, which may be on the fast end of typical recovery. Slower recovery can have a major impact on the system frequency response and can lead to increased load shedding, as seen in Fig. 14-15, and as indicated in Hawaiian Electric's Power Supply Improvement Plan.

A. *Frequency Measurement Time Constant* (T_1)

The time constant T_1 is the time it takes to calculate a valid frequency; overall this should be quick, in the tens of milliseconds range. This time constant is due to the PLL response time and filtering involved to get a valid frequency. Parameter sensitivity of T_1 is in Fig. 16.

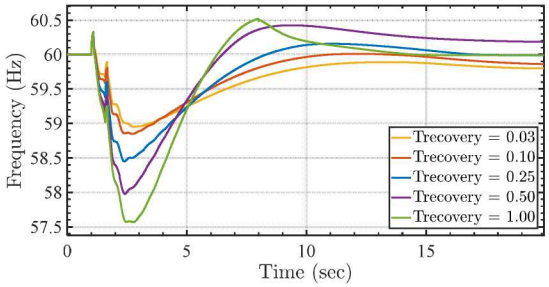

Fig. 14. The system frequency response during a transmission line three-phase fault when PV includes FWVIC and momentary cessation, with different recovery times.

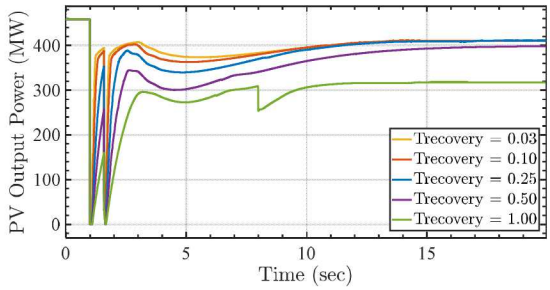

Fig. 15. The power output of the aggregate PV during a transmission line three-phase fault when PV includes FWVIC and momentary cessation, with different recovery times.

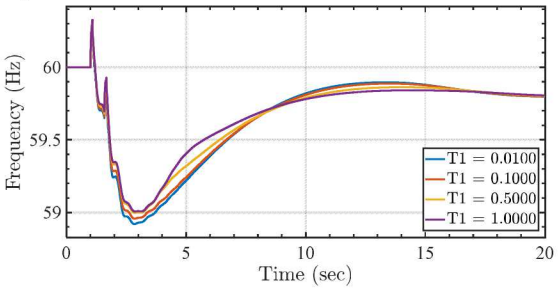

Fig. 16. The system frequency response during a transmission line three-phase fault when PV includes FWVIC and momentary cessation, with different frequency measurement time constants for the control methods.

B. *Virtual Inertia Filter Time Constant* (T_2)

The time constant for the derivative of the frequency needs to be greater than 0.009 in this model to calculate a valid derivative, otherwise the derivative is zero, and the model will behave as the FWC (as seen in Fig. 17 with T_2 = 0.008) rather than the FWVIC. It is suggested to use a derivative constant of 0.01 seconds, because calculation of the derivative should be quick (but constrained by the 0.009 modeling limit).

C. *Inverter Power Time Constant* (T_3)

A faster inverter response time has a significant impact on the frequency nadir during a generation drop as in Fig. 18. As inverter response slows, the control will have less of a positive

impact, especially the virtual inertia potion of the control since the derivative of the frequency changes quickly in comparison to the absolute frequency. Note that if the inverter response time is too slow, it is likely the control may not have a positive impact in all cases.

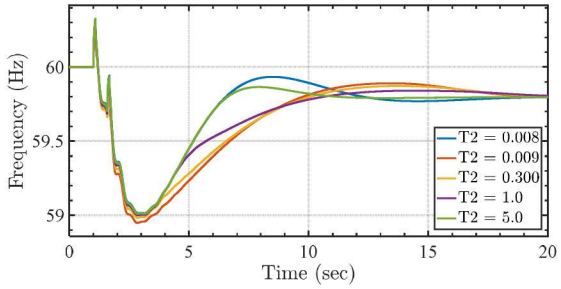

Fig. 17. The system frequency response during a transmission line three-phase fault when PV includes FWVIC and momentary cessation, with different derivative time constants.

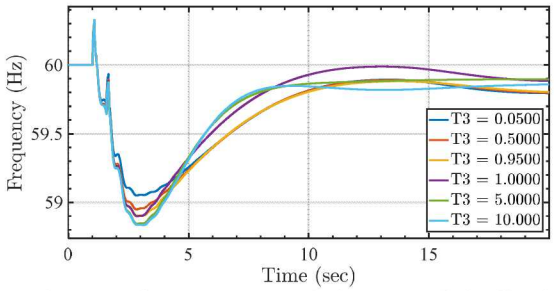

Fig. 18. The system frequency response during a transmission line three-phase fault when PV includes FWVIC and momentary cessation, with different inverter response time constants.

VI. Conclusion

This paper presents and analyzes two smart inverter control models: a frequency-watt method and a hybrid frequency-watt with virtual inertia method. The models also include inverter responses to low voltage conditions, momentary cessation. Custom dynamic models for the two control methods were developed and implemented in PSS\E. The controls are simulated under a three-phase fault contingency on a validated model of the Oahu system. The results indicate a significant improvement in the system response for both smart inverter control methods. Results indicate better performance with reserve margins enabled. Results indicate that if momentary cessation is utilized during faults, a fast recovery time from momentary cessation is necessary to mitigate severe under-frequency events. After this project concluded, the Hawaiian Electric Companies required frequency-watt functionality be activated on inverters interconnected to their systems. The frequency-watt functionality implemented does not include virtual inertia; it does include a deadband of 36 mHz, and a droop of 4% without reserve (i.e. meant for curtailment during load trip events).

Acknowledgement

This work is supported by the US DOE through the Grid Modernization Laboratory Consortium initiative.

The authors would like to thank Hawaiian Electric Company for providing the dynamic model of Oahu Island and for their valuable input to this study.

References

[1] M. Elkhatib, J. Neely, J. Johnson, “Evaluation of fast-frequency support functions in high penetration isolated power systems,” *Proc. IEEE Photovoltaic Specialist Conference*, 2017.

[2] J. Neely, J. Johnson, J. Delhotal, S. Gonzalez, M. Lave, “Evaluation of PV Frequency-Watt Function for fast frequency reserves,” *Proc. IEEE Applied Power Electronics Conference and Exposition (APEC)*, 2016.

[3] A. Hoke, S. Chakraborty, M. Shirazi, E. Muljadi, and D. Maksimovic, “Rapid active power control of photovoltaic systems for grid frequency support,” *IEEE Journal of Emerging and Selected Topics in Power Electronics*, Feb. 2017.

[4] D. Pattabiraman, J. Tan, V. Gevorgian, A. Hoke, C. Antonio, and D. Arakawa, “Impact of Frequency-Watt Control on the Dynamics of a High DER Penetration Power System,” *in IEEE Power and Energy Society General Meeting (PESGM)*, 2018.

[5] J. Johnson, J. Neely, J. Delhotal, M. Lave, “Photovoltaic frequency-watt curve design for frequency regulation and fast contingency reserves,” *IEEE Journal of Photovoltaics*, vol. 6, no. 6, pp. 1611-1618, 2016.

[6] M. Elkhatib, W. Du, R. Lasseter, “Evaluation of inverter-based grid frequency support using frequency-watt and grid forming PV inverters,” *Proc. IEEE Power & Energy Society General Meeting*, 2018.

[7] W. Du, Q. Jiang, M. Erickson, R. Lasseter, “Voltage-source control of PV inverter in a CERTS microgrid,” *IEEE Transactions on Power Delivery*, vol. 29, no. 4, pp. 1726-1734, 2014.

[8] K. Rahimi, A. Tbaileh, R. Broadwater, J. Woyak, M. Dilek, “Voltage regulation performance of smart inverters: power factor versus Volt-VAR control,” *Proc. North American Power Symposium (NAPS)*, 2017.

[9] S. Chakraborty, A. Nelson, and A. Hoke, “Power Hardware-in-the-Loop Testing of Multiple Photovoltaic Inverters’ Volt-var Control with Real-time Grid Model,” in *IEEE Innovative Smart Grid Technologies Conference (ISGT)*, 2016.

[10] J. I. Giraldez Miner et al., “Simulation of Hawaiian Electric Companies Feeder Operations with Advanced Inverters and Analysis of Annual Photovoltaic Energy Curtailment,” National Renewable Energy Lab. (NREL), Golden, CO (United States), NREL/TP-5D00-68681, Jul. 2017.

[11] R. Eriksson, N. Modig, K. Elkington, "Synthetic inertia versus fast frequency response: a definition," *IET Renewable Power Generation*, vol. 12, no. 5, pp. 507-514, 2018.

[12] R. Concepcion, F. Wilches-Bernal, R. Byrne, "Effects of communication latency and availability on synthetic inertia," *Proc. IEEE Power & Energy Society Innovative Smart Grid Technologies Conference (ISGT)*, 2017.

[13] “Rule Number 14.” The Hawaiian Electric Companies, Feb-2018.

[14] A. Hoke et al., “The Frequency-Watt Function: Simulation and Testing for the Hawaiian Electric Companies,” National Renewable Energy Laboratory, NREL/TP-5D00-68884, Jul. 2017.

[15] “IEEE 1547-2018: IEEE Standard for Interconnection and Interoperability of Distributed Energy Resources with Associated Electric Power Systems Interfaces.” IEEE, Apr. 2018.

[16] ““IEEE Standard 1547: Standard for Interconnecting Distributed Resources with Electric Power Systems,” IEEE, Jul. 2003.